

A frictional population model of seismicity rate change

J. Gomberg,¹ P. Reasenber,² M. Cocco,³ and M. E. Belardinelli⁴

Received 25 August 2004; revised 17 January 2005; accepted 21 February 2005; published 22 April 2005.

[1] We study models of seismicity rate changes caused by the application of a static stress perturbation to a population of faults and discuss our results with respect to the model proposed by Dieterich (1994). These models assume a distribution of nucleation sites (e.g., faults) obeying rate-state frictional relations that fail at constant rate under tectonic loading alone, and predicts a positive static stress step at time t_0 will cause an immediate increased seismicity rate that decays according to Omori's law. We show one way in which the Dieterich model may be constructed from simple general ideas, illustrated using numerically computed synthetic seismicity and mathematical formulation. We show that seismicity rate changes predicted by these models (1) depend on the particular relationship between the clock-advanced failure and fault maturity, (2) are largest for the faults closest to failure at t_0 , (3) depend strongly on which state evolution law faults obey, and (4) are insensitive to some types of population heterogeneity. We also find that if individual faults fail repeatedly and populations are finite, at timescales much longer than typical aftershock durations, quiescence follows a seismicity rate increase regardless of the specific frictional relations. For the examined models the quiescence duration is comparable to the ratio of stress change to stressing rate $\Delta\tau/\dot{\tau}$, which occurs after a time comparable to the average recurrence interval of the individual faults in the population and repeats in the absence of any new load perturbations; this simple model may partly explain observations of repeated clustering of earthquakes.

Citation: Gomberg, J., P. Reasenber, M. Cocco, and M. E. Belardinelli (2005), A frictional population model of seismicity rate change, *J. Geophys. Res.*, 110, B05S03, doi:10.1029/2004JB003404.

1. Introduction

[2] Numerous physical models have been proposed to explain observations of large earthquakes causing, or "triggering," an increase in seismicity rate [see Scholz, 1968; Nur and Booker, 1972; Dieterich, 1994; Freed and Lin, 2001; Helmstetter and Sornette, 2002, and references therein]. Aftershocks are the most common such observation, particularly their characteristic temporal signature. Explanation of these observations undoubtedly will tell us something about the physics underlying earthquake failure. In addition to satisfying our scientific curiosity, an understanding of triggering will improve our ability to forecast the probabilities of damaging earthquakes and thus to mitigate earthquake risk.

[3] Among the more popular triggering models is that first proposed by Dieterich [1994], which explains seismicity rate changes as a consequence of frictional failure on a distribution of nucleation sites that has been altered by some (arbitrarily complex) stress perturbation. From this general

formulation he derived an analytic expression for a step increase or decrease in shear stress, which has been widely applied in studies of aftershocks. We refer to this analytic expression as the *Dieterich* [1994] model, and note it as \mathcal{R}_D . In this paper we discuss the assumptions and implications of this model, motivated by its growing application to seismicity studies [e.g., Gross and Kisslinger, 1997; Gross and Burgmann, 1998; Harris and Simpson, 1998; Toda et al., 1998; Gross, 2001; Kilb and Rubin, 2002; Rubin, 2002]. Perhaps a more important motivation from the perspective of social responsibility is that it has been proposed as a key ingredient of strategies for estimating the change in probability of a large earthquake on an individual fault due to a nearby earthquake [Stein et al., 1997; Hardebeck, 2004]. We discuss these strategies by Gomberg et al. [2005].

[4] In this paper we highlight results of a numerical study of the seismicity rate change model proposed by Dieterich [1994]. Some of the results presented revisit previous ones [Gomberg et al., 1997, 1998, 2000], with the intention of providing a clearer presentation and focus on the Dieterich [1994] model. We begin by showing that in some aspects this model is a specific case of a more general one. In part, the specificity comes from invoking a particular frictional response, which depends on the rate of fault slip and evolution of contact properties [Dieterich, 1979; Ruina, 1983]. Moreover, the approach taken by Dieterich [1994] relies on the introduction of a new state variable and corresponding evolution law, which we suggest may ob-

¹U.S. Geological Survey, Memphis, Tennessee, USA.

²U.S. Geological Survey, Menlo Park, California, USA.

³Istituto Nazionale di Geofisica e Vulcanologia, Rome, Italy.

⁴Settore di Geofisica, Dipartimento di Fisica, Università di Bologna, Bologna, Italy.

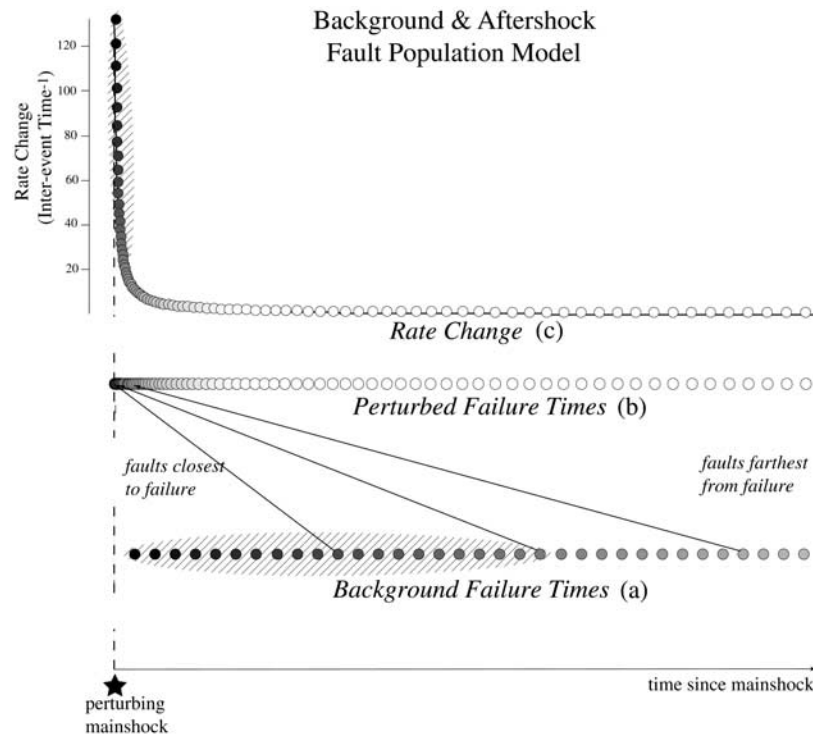


Figure 1. Failure times of a hypothetical population of faults. Although we represent each fault as a spring slider obeying quasi-static rate-state frictional laws (see *Gomberg et al.* [1997, 2000] and Table 2 for details), any physical model in which the faults accelerate toward failure would produce the same results [*Gomberg et al.*, 2000]. (a) Failure times of faults being loaded and failing at a constant rate. Each circle represents a fault that will fail at a time corresponding to the circle's position on the horizontal axis. A step increase in stress occurs at time t_0 (dashed vertical line). Shading of circles indicates how mature or close to failure a fault was just prior to t_0 (darker shading indicating faults closer to failure at t_0). The most mature faults are indicated by hachured oval. (b) Failure times of the same faults advanced by the positive stress step. The amount of advance depends on the fault's maturity at t_0 . The most mature faults now fail within a much shorter time as indicated by the hachured oval containing the same set of failure times in all frames. Although much clearer in Figure 1c, the oval is much more compressed along its time axis in Figures 1b and 1c. (c) Seismicity rate, or inverse of the interevent times. Hachured oval contains the interevent times or rates for the same faults indicated by ovals in Figures 1a and 1b. Curved line is the rate predicted by the *Dieterich* [1994] model.

secure the underlying physical processes. Next we show that the precise form of the frictional response assumed in the *Dieterich* [1994] model has significant effect on the predicted seismicity rate change. We then go beyond our previous work and examine assumptions about the diversity of characteristics among the faults composing the model population. We also look at timescales much longer than those addressed by *Dieterich* [1994], focusing on the implications of assuming faults fail repeatedly and are finite in number.

2. A General Model for Seismicity Rate

[5] Here we consider the change in seismicity rate produced when a stress change is applied to a population of faults that have been undergoing constant rate tectonic loading. While our illustrations consider populations of discrete nucleation sources or faults, in part because it is easier conceptually [e.g., *Dieterich*, 1994, Figure 1; 1987], the results also apply to continuous distributions amenable

to use in probability calculations. To help with keeping track of the various relevant time parameters in the models presented in this and *Gomberg et al.* [2005], we list them in Table 1. In order to illustrate basic concepts, we first explore an extremely simple model in which all the faults in the population have identical frictional properties (Table 2) and are governed by the same frictional laws. The only difference between faults is how mature each one is at any time (i.e., how much time has passed since each fault last failed). The faults do not interact with one another. If the fault maturities are equally spaced, then in the absence of stress transfer the population as a whole produces earthquakes at a constant rate, $r = 1/\delta$, where δ is the time between successive earthquakes (Figure 1a). If a perturbing earthquake occurs at time t_0 and generates a stress step (positive, or failure encouraging, in this example), subsequent earthquakes occur in the population sooner than they otherwise would have (we say that they are “clock advanced”). The rate of earthquakes increases if the magnitude of the clock advance on a fault decreases with increasing fault maturity

Table 1. Time Parameters in the Models Presented in This Paper and by *Gomberg et al.* [2005]

Symbol	Background/Aftershock Seismicity	Single Fault Failure Probability
t_0	time when static stress step is applied	
δ	time interval between successive earthquakes on different faults	
T	recurrence time, or time interval between failures	
T'	perturbed recurrence time	
s	time of the last earthquake	0
m	maturity at t_0 , $t_0 - s$	
t_c	clock advance, change in recurrence time	
t	elapsed time since the application of the stress perturbation, $T' - t_0$	
t_e		elapsed time

Description of time parameters employed in our model of seismicity rate change for a population of faults, as in background and aftershock seismicity (middle column), and as they relate to the failure probability of a single fault (right column), discussed by *Gomberg et al.* [2005]. For the seismicity rate change application, unless specified otherwise, absolute or interval times refer to an individual fault in the population. Times (not interval times) are absolute, all relative to the same arbitrary origin. For the single fault failure probability application, times are relative to the time of the last earthquake.

[see, e.g., *Gomberg et al.*, 2000]. These clock advances produce a “pileup” of failures immediately after t_0 (Figure 1b), shortened interevent times, and increased seismicity rate (Figure 1c). The greatest contribution to the rate increase is associated with earthquake on the faults that had been closest to failure at t_0 . These ideas also are illustrated by of *Dieterich* [1994, Figure 1]. Note that although our Figure 1 was produced using a frictional model of failure for each fault, the results apply to any model in which faults accelerate toward failure [*Gomberg*, 2001]. To gain insight into the way the seismicity rate in such a system responds to the stress step, we shall follow the timing of individual earthquakes on individual faults in the model.

[6] We first describe this idealized fault population mathematically. As noted in Table 1, we define T_n as the recurrence interval (the time between failures), hereafter referred to as recurrence interval, of the n th fault in the population and s_n as the time of the last earthquake on fault n (i.e., the start of current cycle on fault n). (Note that in all the numerical models presented in this study the recurrence intervals (also called cycle times in other studies) we calculate differ from those predicted by fully dynamic failure models. This is because we compute failure times using a quasi-static model for initial conditions at time s_n (see Table 2) that are not exactly those characterizing the system at the time of the last earthquake. This difference has almost no effect on the numerically modeled rate changes at short timescales (times $\ll T_n$) and thus on most of the results we present. It does affect the quantitative aspects of the model presented in section 4, but we interpret the model qualitatively only to illustrate more general implications. The index n also indicates the order of occurrence of earthquakes in the population.) We omit the subscripts in Table 1 so that the relevant variables apply to models in both this and *Gomberg et al.* [2005]. If the population is composed of identical faults (i.e., all sources have identical constitutive properties and initial conditions) T_n is the same for all faults; therefore we initially assume that the recurrence interval is constant, but later we consider the possibility that different faults have different T_n . The time of the next failure of fault n will be $s_n + T_n$. Similarly, failure of the

$(n-1)$ th fault occurs earlier at $s_{n-1} + T_{n-1}$. The interevent time (interval between two subsequent events on two distinct faults) is

$$\delta_n = T_n - T_{n-1} + s_n - s_{n-1} \quad (1)$$

in which $s_n > s_{n-1}$ and the instantaneous seismicity rate is $r_n = 1/\delta_n$.

[7] Now consider the effect of a perturbing stress step applied to all faults in the population, produced by a large earthquake occurring at time t_0 ($t_0 > s_n$). For accelerating failure models, the clock advance on fault n depends on the fault’s maturity, $m_n = t_0 - s_n$ [*Dieterich*, 1994; *Gomberg et al.*, 2000; *Gomberg*, 2001; *Belardinelli et al.*, 2003]. The perturbed interevent time becomes

$$\delta'_n = T'_n - T'_{n-1} + s_n - s_{n-1} \quad (2)$$

where $T'_n = T'_n(m_n)$ and $T'_{n-1} = T'_{n-1}(m_{n-1})$ are the perturbed recurrence intervals on faults n and $n-1$, respectively, which depend on the maturities of the respective faults. The perturbed seismicity rate is $r'_n = 1/\delta'_n$, which also depends on the maturities of both faults.

Table 2. Model Parameters Used to Compute Figures 2 and 4^a

Parameter	Value
A	0.005
B	0.010
μ_0	0.7
d_c	1 mm
Stiffness k	0.05 m s ⁻¹
Reference velocity V_0	10 ⁻⁹ m s ⁻¹
Failure velocity V_f	0.1 m s ⁻¹
Tectonic loading velocity V	10 ⁻⁹ m s ⁻¹
Initial velocity V_{init}	10 ⁻⁹ m s ⁻¹
Initial stress (friction) as negative percent from stable friction μ_{init}	-10%
Perturbation amplitude	0.5 m

^aSee *Gomberg et al.* [1997, 2000] for explanation. If the normal stress is $\sigma = 10$ MPa, these parameters become stiffness 0.5 MPa m⁻¹, stress step amplitude $\Delta\tau = 0.25$ MPa, tectonic stressing rate 5×10^{-10} MPa s⁻¹ = 0.016 MPa yr⁻¹; these parameters scale linearly with σ .

Since we have assumed that all faults have identical constitutive properties and initial conditions (although the absolute times, s_n , differ), and thus have the same unperturbed recurrence intervals (i.e., $T_n = T_{n-1}$ in equation (1)), then the perturbed interevent time becomes

$$\delta'_n = \delta_n + T'_n - T'_{n-1} \quad (3)$$

In section 5 we examine the case in which the faults in the population have different constitutive properties (i.e., unequal recurrence intervals). It is important to note that in this population model of seismicity rate change, the distribution of T_n and s_n within the population determine both the background seismicity rate (when no perturbation is applied) and the seismicity rate change caused by a stress step. Our model simulates a constant background seismicity rate simply by assuming a constant T_n (i.e., a population of identical faults) and values of s_n distributed evenly at equal time intervals within the population.

[8] Although we have not assumed any particular failure mechanism in the discussion so far, equation (3) provides insight into how a perturbing earthquake changes the seismicity rate. Advancing the failure times (or decreasing the recurrence intervals) does not necessarily increase the population's seismicity rate. In particular, the interevent time and seismicity rate remain constant if the recurrence intervals on all faults are perturbed by the same amount. This is the case for immature (far from failure) frictional faults, that is, if $T'_n = T'_{n-1}$, then $\delta'_n = \delta_n$ and $r'_n = r_n$. For the seismicity rate to increase (interevent time to decrease), the perturbed cycle time must be greater for the more mature faults than for faults farther from failure (i.e., $T'_{n-1} > T'_n$ in equation (3) or $dT'/dm > 0$ [see also *Gomberg et al.*, 1998, Figure 3b]).

[9] Equation (3) is a general formula for the seismicity rate and from it an equally general relation for the change in seismicity rate due to some perturbing stress can be derived [see also *Gomberg et al.*, 2000; *Beeler and Lockner*, 2003; *Gomberg et al.*, 2005]. This general relation can be turned into analytic expressions if, for a given type of stress perturbation (which theoretically can have any time history), the relationship between recurrence interval change and fault maturity is known (or assumed). Indeed, the *Dieterich* [1994] seismicity rate change model can be derived using this approach. Here we summarize the derivation of this general rate change and show in more detail how it leads to the *Dieterich* [1994] model, \mathfrak{R}_D , in Appendix A. The change in recurrence interval or clock advance is $t_c(m_n) = T_n - T'_n$, which as noted, depends on the fault's maturity. If we let $\Delta t_c(m_n) = t_c(m_n) - t_c(m_{n-1})$, then we can rewrite equation (3), and thus the rate change, in terms of the dependence of the clock advance on maturity. Recalling that the unperturbed recurrence times are the same on all faults, or $T_n = T_{n-1}$, equation (3) can be written as

$$\begin{aligned} \delta'_n &= \delta_n + T'_n - T'_{n-1} = \delta_n + T'_n - T'_{n-1} - T_n + T_{n-1} \\ &= \delta_n - \Delta t_c(m_n) = \delta_n \left[1 - \frac{\Delta t_c(m_n)}{\delta_n} \right] \end{aligned} \quad (4a)$$

Noting that $\delta'_n/\delta_n = r_n/r'_n$ and the definitions of δ_n in equation (1) with $T_n = T_{n-1}$ and maturity as $m_n = t_0 - s_n$,

then $\delta_n = \Delta s_n = -\Delta m_n$ and we can write the rate change as

$$\frac{r'_n}{r_n} = \left[1 + \frac{\Delta t_c(m_n)}{\Delta m_n} \right] \quad (4b)$$

Since in this model the unperturbed recurrence intervals are constant $\Delta t_c(m_n) = -\Delta T'_n$ and, using differentials instead of differences, the instantaneous rate change becomes

$$\frac{r'_n}{r_n} = \frac{1}{1 - \frac{dT'_n}{dm_n}} \quad (4c)$$

[10] We show in Appendix A how an analytic expression for the derivative in equation (4c) can be obtained, yielding \mathfrak{R}_D when substituted into equation (4c). Summarizing the derivation, determination of an analytic solution to equation (4c) requires an analytic description of the response of a single fault to a stress perturbation. To obtain \mathfrak{R}_D , we use the description derived by *Gomberg et al.* [1998] of how the recurrence interval (or clock advance) depends on maturity and a perturbation applied at time t_0 . In this aftershock model the time of the last failure of each fault, s_n , differs for each fault and t_0 is a single time, all measured relative to some arbitrary origin. The identical distribution of maturities, $m_n = t_0 - s_n$, would result by shifting s_n to be the same for all faults, and considering t_0 to vary for each fault, so that the derivative in equation (4c) becomes

$$\frac{dT'_n}{dm_n} = \frac{dT'_n}{dt_0} = \left[1 - e^{-\Delta\tau/A\sigma} \right] e^{-t/t_0} \quad t_0 = \frac{A\sigma}{\dot{\tau}} \quad (5)$$

where $t = T'_n - t_0$ represents the time that has passed since the application of the stress perturbation (i.e., the “triggering delay” [*Belardinelli et al.*, 1999, 2003]), $\Delta\tau$ is the amplitude of the shear stress step, σ is the ambient effective normal stress, $\dot{\tau}$ is the tectonic stressing rate, and A is an empirical frictional parameter. If the background rate is assumed to be constant, as in the work by *Dieterich* [1994], substitution of equation (5) into equation (4c) results in the *Dieterich* [1994] model,

$$\mathfrak{R}_D(t) = r'/r = \left\{ \left[e^{-\Delta\tau/A\sigma} - 1 \right] e^{-t/t_0} + 1 \right\}^{-1} \quad (6)$$

The predictions of this model agree very well with the numerically calculated rate change of Figure 1c. This should not be surprising because the numerical example shows that it is the most mature faults that give rise to the rate change. These are precisely the “self-accelerating” faults that *Dieterich* [1994] assumed are most significant and justifies the approximation he makes in developing his analytic model (which explicitly neglects all faults earlier in their cycles). Note that the less mature faults are all clock advanced, but all by nearly the same amount (i.e., $T_n = T_{n-1}$) so that their failure rate does not change.

[11] Equation (4c) is a general expression for rate change that relies on the simple idea that seismicity rate change is measured by the change in interevent time, which depends on how the recurrence interval or failure time changes with

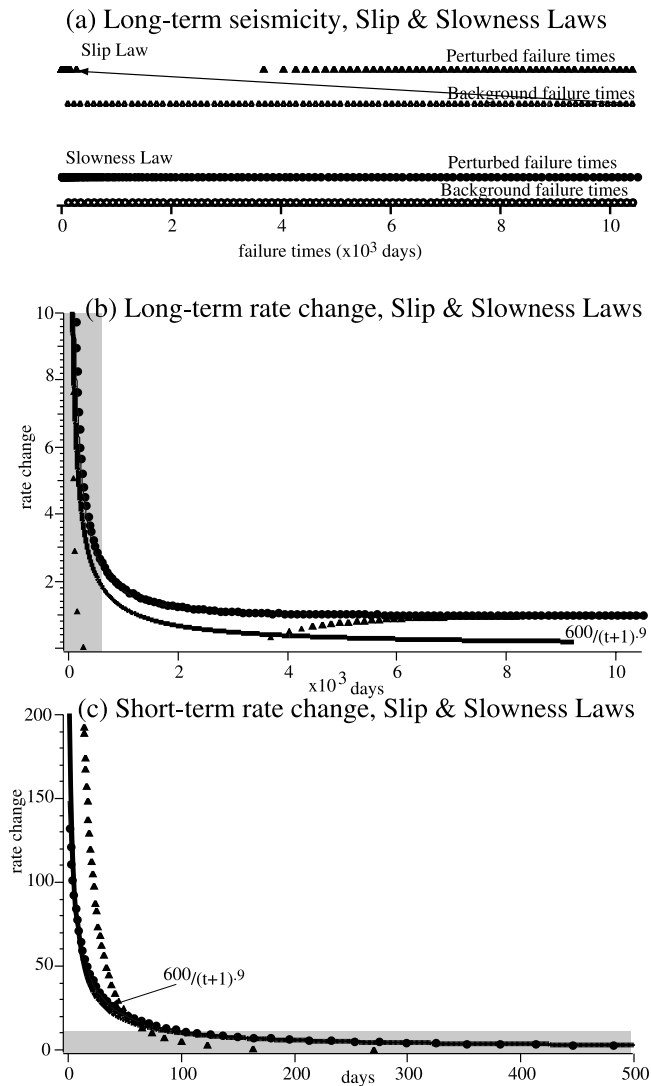


Figure 2. (a) Background and advanced failure times for populations of identical faults (same as population shown in Figure 1) obeying the slowness law (circles) and slip law (triangles). The perturbing stress step is the same as in Figure 1. Note that the advanced failure times pileup much more for the slip law. Arrow connects the same fault under background and perturbed stressing. (b) Rate changes, normalized to the background rate, derived from the interevent times of the slip law (triangles) and slowness law (circles) populations as functions of time from the main shock. *Dieterich's* [1994] model is shown by thin black curve. An Omori decay model (thick black curve) fits the slowness law rate change model predictions better than it does the slip law model. The Omori decay model shown was fit by trial and error to best match both the slip and slowness law predictions (and thus does not decay with a value of $p = 1$.) The slip law model predicts a faster and deeper rate decrease that temporarily drops below the background rate. Vertical shaded area corresponds to time period shown in Figure 2c. (c) Same models shown for a shorter time range than in Figure 2b. Horizontal shaded area corresponds to rate change range shown in Figure 2b.

fault maturity. We suggest that applying it to derive \mathcal{R}_D (equation (6)) provides a clear connection to the underlying physical system. Indeed, application of \mathcal{R}_D requires knowledge of fewer parameters and computations than a numerical solution of equation (4c). However, the simplicity of the analytic solution comes at the price of needing to validate the assumption of self-accelerating slip on all sources, and at a loss of generality as it requires that state (in this case a measure of contact properties) evolves according to the slowness law [see *Beeler et al.*, 1994] and that the perturbation is a stress step. For most general perturbations both the solution to equation (4c) and the procedure outlined by *Dieterich* [1994] for finding rate change are numerical. (One exception is an analytic solution for a transient perturbation with a boxcar time function derived following the same recipe as for the *Dieterich* [1994] model in Appendix A but instead using the transient “load function” of *Gomberg et al.* [1998].) Equation (4c) also permits rate changes to be derived for alternative failure mechanisms, and in some cases analytic expressions may be found. One example is illustrated by *Gomberg* [2001] in which a rate change formula is derived for faults failing according to the theory of subcritical crack growth. Finally, as discussed by *Beeler and Lockner* [2003] and *Gomberg et al.* [2005, equation [4c]] may be considered as a probability density function and used directly to estimate changes in conditional failure probabilities.

3. Frictional Response Matters

[12] The *Dieterich* [1994] model assumes that the evolution of fault contact properties, or “state,” may be described by a relation often referred to as a “slowness” law [see *Beeler et al.*, 1994]. The slowness law defines the temporal evolution of a state variable that accounts for the changing properties of the surface contacts. It represents one possible realization of the evolution equation, which is one of the two constitutive relations defining the rate and state frictional formulation. We find that the seismicity rate change depends strongly on how state evolves, i.e., on which state evolution law faults obey. Figure 2 compares rate changes calculated numerically for the slowness law and another commonly invoked state evolution relation, the slip law [see *Beeler et al.*, 1994], on two timescales to emphasize the differences.

[13] Again, for illustrative purposes we employ the simple seismicity model described in section 2. Immediately after the perturbing stress, the slip law predicts a rate change that is larger and decays more rapidly than that predicted by the slowness law. The rate for the slowness law may be fit by the modified Omori law, in which the rate of earthquakes decreases with time as an inverse power law

$$dN/dt = K/(t + c)^p \quad (7)$$

in which N is the cumulative number of earthquakes and K , c , and p are empirical constants [Utsu, 1961]. The longer-term behaviors of the rate changes for these two state evolution laws also differ significantly. The slip law predicts a small quiescence following the initial rate increase, which may last for years. The observational evidence for or against such quiescence is mixed. *Ziv et al.* [2003] and *Ogata et al.*

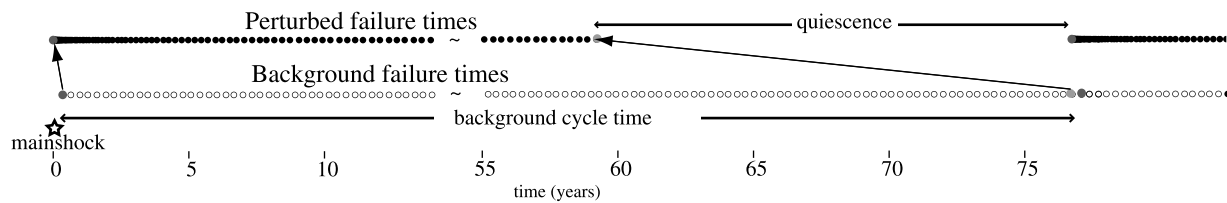


Figure 3. Simulated seismicity for the same population of identical faults shown in Figure 1 but for a longer time window that includes failures of all the faults in the finite population ($N = 200$ in this example). Note change in timescale. Arrows connect the failure times one fault (fault N) in the unperturbed and perturbed states. In this example, the unperturbed cycle time is 76.86 years and the clock advance for faults far from failure is 17.56 years, which results in a quiescence period of 17.56 years. The Coulomb clock advance for this example is 15.86 years. The greater frictional clock advance is consistent with the results of *Gomberg et al.* [2000].

[2003] find evidence for quiescences following major earthquakes, beginning several months after the main shock and lasting for years. *Toda and Stein* [2003] also provide a list of studies in which quiescences have been measured. Other recent studies suggest that quiescences are rare, particularly relative to predictions of Coulomb stress modeling that predict rate changes that correlate with the magnitude and sign of the stress changes [*Felzer et al.*, 2003; *Marsan*, 2003]. These studies examine rate decreases inferred by others and show that they may be analysis artifacts. They interpret the paucity of rate decreases as a possible indication that dynamic triggering may promote only rate increases, that stress change patterns are more complex than the models predict, or that the seismicity response to stress changes is asymmetric with respect to the sign of the stress change.

[14] Differences in predicted rate changes between the slip and slowness laws were also noted by *Gomberg et al.* [2000]. As they explained, a positive stress step causes an abrupt increase in slip velocity. The slip law model predicts a sharp rate increase followed by quiescence because strengthening only occurs when the fault is slipping in some intermediate velocity range and weakening occurs above this range. For the most mature, fastest slipping faults, the increased velocity causes these faults to weaken rapidly and fail almost immediately. The velocity of slower slipping, less mature faults is elevated into the strengthening range, causing them to decelerate and resulting in quiescence. The slip velocities of the least mature faults at the time of the stress step are sufficiently low that there is little frictional effect and the rate does not change. The slowness law has a much smoother dependence on maturity (i.e., slip velocity in this context) and a correspondingly smoother rate change results.

4. Implications of Recycling Sources

[15] The formulation of *Dieterich* [1994] assumes that sources do not fail more than once, which implies that there is (in the model) an infinite population of sources. In contrast, our model allows repeated failure of sources. *Dieterich* [1994] also assumes that all sources are mature, or near failure (experiencing self-accelerating slip). It follows that the response of a source to a stress perturbation depends on those properties of the source that control failure, but not on how long it took the source to reach

failure. In contrast, our model considers the importance of a source's maturity in its response to a stress perturbation. For time intervals short compared to typical source recurrence intervals, these differences appear to have insignificant impact, as evidenced by the close agreement between the rate change we obtain numerically and that obtained by *Dieterich* [1994] (Figure 1). We examine the possible implications of these model differences for longer-timescale calculations. We acknowledge that the *Dieterich* [1994] model was not developed for this purpose, but believe that such a comparison may still be instructive for understanding the implications of the respective sets of assumptions and the limitations of each model.

[16] We consider what happens when sources in a finite population each recur quasiperiodically. The assumption of quasiperiodic recurrence underlies many probabilistic models of earthquake occurrence, consistent with observations of large to very small earthquakes [see *Matthews et al.*, 2002, and references therein]. To explore the implications of assuming that the source population is finite, we return to the simple population used for Figures 1 and 2 and interpret only the most general features of its behavior. (Although highly simplified, adoption of a nearly identical model of recurring clusters by *Meade and Hager* [2004] lends it credibility.) The maturity of sources in the population is assumed to be distributed evenly at equal time intervals. Recall that a main shock-generated stress step clock advances the failure times of the faults close to failure, causing a pileup of failures and an immediate increase in failure rate (Figure 3). Faults farther from failure have larger but nearly equal clock advances, so that the failure rate at later times is only minimally affected. In this context, the fact that the number of faults, N , is finite means that a quiescence (a reduced or zero rate) must occur after the failure of the N th fault (Figure 3). The clock advance for the faults farthest from failure is approximately equal to the Coulomb clock advance $\Delta\tau/\dot{\tau}$. Hence the duration of the quiescence is approximately equal to the Coulomb clock advance. In reality, the duration of quiescence will vary, depending on the particular distribution of source maturity (which may not be distributed evenly at equal time intervals, as we have assumed) at the time of the perturbing earthquake, the true complexity of failure processes, and source interactions. (Preliminary fully dynamic calculations indicate that the recurrent nature of the failure pattern may be more complex than these quasi-static models predict.)

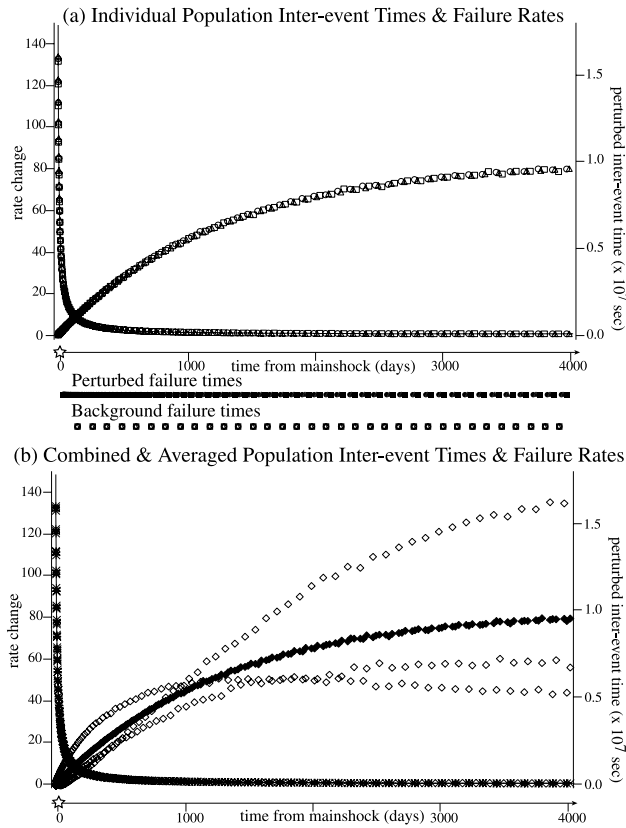


Figure 4. (a) Below time axis, the failure times for three subpopulation of faults under tectonic loading alone (“background state”) are shown by open squares, triangles, and circles and, with the addition of a positive stress step at $t = 0$ (“perturbed state”), by corresponding solid symbols. The faults within each subpopulation have identical cycle times (but differing maturities). Cycle times differ between subpopulations. Above time axis, interevent times and failure rate change are shown for each subpopulation. The dependence of interevent time and failure rate on the delay time (time from the main shock) is the same in each subpopulation. The cycle times are altered by changing d_c to 0.01 m in one case (triangles, cycle times 69.0 years), and B to 0.02 in another (squares, cycle times 130.7 years). For the reference case (circles, cycle time 76.9 years) $d_c = 0.001$ m and $B = .01$. (b) Interevent times (open diamonds) are highly variable for a population of faults containing all three fault types shown in Figure 4a. However, interevent times averaged over three samples vary smoothly with delay time (solid diamonds). The inverse of these averages, or the averaged seismicity rate change (asterisks), is identical to that of the individual fault populations in Figure 4a. The solid curve through the numerically calculated rate changes is the *Dieterich* [1994] model.

[17] In summary, a positive stress perturbation in a finite source population creates a pattern of increased failure rate, waning failure rate, and then zero failure rate (the population becomes quiescent). Curiously, the effect of the stress perturbation in this model endures well beyond the quiescence (theoretically forever!). As tectonic loading continues, this pattern repeats (Figure 3) unless perturbed by another transient stress change (e.g., another main shock).

We expect our model of recycled sources, and thus finite source populations, to be most relevant to the case in which the minimum magnitude of observed earthquakes is relatively large. Albeit overly simple, this model may explain some observations of repeated clustering of large earthquakes (e.g., as documented by *Pollitz et al.* [2003] and *Meade and Hager* [2004]).

5. Effects of Frictional Heterogeneities

[18] What happens if, contrary to our assumptions thus far, faults in the population are not identical? We show that the rate change is still predictable on average, even if the background rate fluctuates and the population is composed of faults having differing constitutive properties but all obeying the same frictional laws. Since we are concerned only with the temporal behavior of the failure process, the only relevant individual fault properties are those that determine the background and perturbed cycle times. For a rate-state frictional model these properties include empirical constitutive parameters A and B , the length scale parameter, d_c , the material stiffness, and initial conditions in a quasi-static model. We simulate seismicity for a population of faults composed of a mixture of three different homogeneous subpopulations, one of which we showed in the previous examples. These subpopulations are characterized by differing constitutive parameters d_c and B and thus by differing recurrence intervals. However, the distributions of perturbed interevent times and failure rates in each subpopulation are identical (Figure 4). This apparent lack of dependence on constitutive parameters d_c and B (and thus the recurrence intervals, which may be viewed as proxies for constitutive properties), further validates the assumptions underlying the *Dieterich* [1994] model (i.e., equation (5) does not depend on these parameters). As noted in section 4, this should not be surprising because the response to a stress perturbation of sources that are near

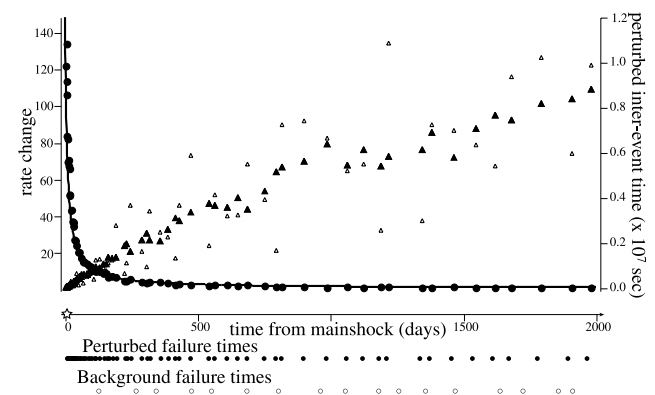


Figure 5. Below time axis, failure times for a population of faults with identical cycle durations but randomized cycle start times (coefficient of variation is 0.25), under tectonic loading alone (background case, open circles) and with the addition of a positive stress step (main shock) at $t = 0$ (perturbed case, solid circles). Above time axis, interevent times (open triangles) are averaged with a moving window (solid triangles) and inverted to estimate the rate change (solid circles). The solid curve shows rate changes predicted by the rate-state seismicity rate change model.

failure depends only on the properties that control failure and not on how long it took for these sources to reach the near-failure state.

[19] While real populations contain faults with a variety of properties, we only can observe the failure times of an entire population. Although combining these three homogeneous subpopulations into one resulted in background interevent times that are no longer constant and perturbed interevent times that no longer vary smoothly (Figure 5), averaging the interevent times over a time window long enough to include a failure of each type of fault results in a rate change that varies in exactly the same way as the individual single-fault populations. Similarly, if the background rate is only constant over some smoothing timescale, then the seismicity rate change remains predictable. (The averaging window must be at least as long as the interevent time of the population with the slowest background rate, or longest interevent time, which in this particular example is ~ 11.6 days.) Next we illustrate these ideas with a numerical example in which we perturb the cycle start times of a population of identical faults randomly about some constant background failure rate. If the random variability is removed by averaging interevent times over an appropriate window, the rate change remains predictable on average (Figure 5).

6. Conclusions

[20] We have examined in some detail some of the assumptions and predictions of the analytic *Dieterich* [1994] model of seismicity rate change, \mathcal{R}_D . *Dieterich* [1994] considers the general case of how seismicity may be affected by a stress perturbation of arbitrary complexity, modeling seismicity as a distribution of nucleation sources obeying specific frictional laws. We focus on his analytic model for the response of seismicity to a stress step, which has been widely applied to explain the temporal behavior of aftershocks. When viewed as an aftershock model, the sources naturally may be considered as a specific population of faults that obey rate-state frictional relations and that fail at constant rate under tectonic loading alone. \mathcal{R}_D predicts that a positive static stress step at time t_0 causes an immediate increase in seismicity rate that decays inversely with time, as predicted by Omori's law.

[21] \mathcal{R}_D may be derived from simple general ideas, which we demonstrate using both numerically computed synthetic seismicity and a simple mathematical formulation for seismicity rate. These demonstrations show that simply advancing the failure times (clock advancing) does not change the seismicity rate unless the clock advances depend on fault maturity in a particular way. The mathematical formulation leads to a simple expression for seismicity rate change that can be computed numerically or in some cases used to derive an analytic expression, given a known relationship between failure time and fault maturity. This formulation is general in the sense that it applies to any failure mechanism and stress perturbation time history. For one particular laboratory-based failure relation, it leads to \mathcal{R}_D . Finally the synthetic seismicity and the mathematical formulation show that the largest seismicity rate increase is associated with the faults closest to failure at the time t_0 of the static stress step. This results validates an assumption of the

Dieterich [1994] model that explicitly includes only faults that are already close to failure at t_0 .

[22] Numerically computed seismicity rate changes show that the model predictions depend strongly on how state evolves, i.e., on which state evolution law faults obey. In particular, assumption of a slip state evolution law, rather than the slowness law assumed in the *Dieterich* [1994] model, leads to larger predicted rate increases with faster decay, followed by a quiescent period. This result suggests that observations of seismicity rate changes could be used to identify the more realistic set of frictional relations.

[23] We examine the implications of assuming that faults fail repeatedly and regularly, and thus that a population of faults is finite. Although these represent alternatives to the assumptions made in the *Dieterich* [1994] model, they matter only for timescales much longer than he considered. If the fault population is finite, quiescence must result after a seismicity rate increase, regardless of the specific frictional relations. For the simple models we examined, in which the fault maturities are distributed over the recurrence interval, the duration of the quiescence would be of the same order as $\Delta\tau/\bar{\tau}$ and occur after a time that depends approximately on the average recurrence interval of the faults in the population. Additionally, in the absence of any new load perturbations the pattern of rate increase followed by quiescence should approximately repeat. This model behavior may provide a simple explanation for why the clustering of large earthquakes often repeats, without relying on intercluster event interactions or other complexities.

[24] The *Dieterich* [1994] model assumes that a constant background rate exists. We show that the rate change is still predictable on average even if the background rate varies and the population is composed of faults having a range of constitutive properties but obeying the same frictional laws.

Appendix A

[25] The *Dieterich* [1994] rate change model, \mathcal{R}_D , may be derived from equation (4c), as well as expressions of *Gomberg et al.* [1998]. To do this, we must find an analytic expression for the derivative, dT'/dm , which for the case of this fault population model equals dT'/dt_0 (see the text surrounding equation (4c)). This describes how the cycle time, T'_n , changes with respect to the time of the perturbing stress, t_0 . This can be done for an approximate rate-state frictional model. The derivation of the equations originates with the frictional failure criterion that failure occurs when the slip velocity becomes large. The cycle time is the duration required to go from an initial velocity, V_s , (which embodies the starting conditions) to the velocity at failure. As in the work by *Dieterich* [1994], *Gomberg et al.* [1998] also derive an expression for the slip velocity of a fault near failure obeying a quasi-static rate-state frictional law (their equation (10b)). The failure or cycle time may be found by defining failure as when the velocity becomes infinite, which happens at the time that makes the denominator of equation (10b) zero, resulting in

$$T' = t_a \{ \ln[\dot{\tau}/\sigma\gamma V_s - L] - \Delta\tau/A\sigma \} \quad t_a = A\sigma/\dot{\tau} \quad (A1a)$$

(Because failure occurs within such a short duration, the difference is insignificant between an infinite failure

velocity and some finite rupture velocity.) L is a load function that depends on the type of stress perturbation [see *Gomberg et al.*, 1998, Table 2] and the time of the perturbation, t_0 . Here we use slightly different notation than by *Gomberg et al.* [1998] (e.g., $\dot{\tau}/\sigma = \dot{\mu}_b$, $\Delta\tau/\sigma = B$, $A = a$), and γ combines some of the constitutive parameters [see *Gomberg et al.*, 1998, equation (7)]. In the absence of any perturbation the unperturbed cycle time can be computed from equation (A1a) with $L = -1$ and $\Delta\tau = 0$, or

$$T = t_0 \left\{ \ln \left[\frac{\dot{\tau}}{\sigma\gamma V_s} + 1 \right] \right\} \quad (\text{A1b})$$

The load function L is defined for a stress step in Table 2 of *Gomberg et al.* [1998] as

$$L = e^{(\dot{\tau}t_0/A\sigma)} \left[1 - e^{(\Delta\tau/A\sigma)} \right] - 1 \quad (\text{A2})$$

[26] The derivative, dT'/dt_0 , from equation (A1a), becomes

$$\frac{dT'}{dt_0} = - \left[\frac{A\sigma}{\dot{\tau}} \right] e^{(\Delta\tau/A\sigma)} e^{(\dot{\tau}T'/A\sigma)} \frac{dL}{dt_0} \quad (\text{A3})$$

Taking the derivative of L with respect to t_0 , substituting the result into (A3), and making the change of variables $t = T - t_0$ yields the needed derivative

$$\frac{dT'}{dt_0} = \left[1 - e^{-\Delta\tau/A\sigma} \right] e^{-t/t_0} \quad (\text{A4})$$

We see that use of equation (A4) in equation (4b) results in the *Dieterich* [1994] rate change model

$$\mathfrak{R}_D = \frac{r'}{r} = \left\{ 1 - \frac{dT'}{dt_0} \right\}^{-1} = \left\{ \left[e^{-\Delta\tau/A\sigma} - 1 \right] e^{-t/t_0} + 1 \right\}^{-1} \quad (\text{A5})$$

Finally, for completeness and as background for *Gomberg et al.* [2005] we derive \mathfrak{R}_D as it applies to estimating the probability of failure of a single fault. We consider a set of potential earthquake failure times t_f and number of events, n , to define an earthquake rate $r(t_f) = \Delta n/\Delta t_f$. Since we now consider a single fault, $\Delta n = 1$, the failure time equals the cycle time, or $t_f = T$ and all potential failure or cycle times are measured relative to the time of the last earthquake. Letting $\delta' = \Delta T'$, $\delta = \Delta T$ in equation (4a) or noting that $T' = T - t_c$, we can write

$$\Delta T' = \Delta T \left[1 - \frac{\Delta t_c}{\Delta T} \right] \quad (\text{A6a})$$

Again using differentials instead of differences, the rate change becomes

$$\mathfrak{R}_D = \frac{r'}{r} = \frac{\Delta T'}{\Delta T} = \frac{1}{\left[1 - \frac{dt_c}{dT} \right]} \quad (\text{A6b})$$

As for the aftershock population model, the derivative in equation (A6b) also describes how the cycle or failure time

changes with fault maturity, since for a perturbation applied at some t_0 (now measured from the time of the last earthquake) a longer cycle time means a fault will be less mature (farther from failure) than for one with a shorter failure or cycle time. Equations (A1a) and (A1b) can be combined to find the analytic expression for dt_c/dT , which yields exactly the same expression for the rate change as equation (A5).

[27] **Acknowledgments.** The authors thank Warner Marzocchi, Karen Felzer, Teruo Yamashita, Francis Albaredo, Sandy Steacy, Ned Field, Jim Dieterich, Ross Stein, and Jeanne Hardebeck for their thoughtful reviews. We give a special thanks and acknowledgment to Nick Beeler, who contributed many ideas and much sweat to this work. M.E.B. gratefully acknowledges the financial support from U.E. under contract EVG1-2002-00073 (PREPARED).

References

- Beeler, N. M., and D. A. Lockner (2003), Why earthquakes correlate weakly with the solid Earth tides: Effects of periodic stress on the rate and probability of earthquake occurrence, *J. Geophys. Res.*, *108*(B8), 2391, doi:10.1029/2001JB001518.
- Beeler, N. M., T. E. Tullis, and J. D. Weeks (1994), The roles of time and displacement in the evolution effect in rock friction, *Geophys. Res. Lett.*, *21*, 1987–1990.
- Belardinelli, M. E., M. Cocco, O. Coutant, and F. Cotton (1999), Redistribution of stress during coseismic ruptures: Evidence for fault interaction and earthquake triggering, *J. Geophys. Res.*, *104*, 14,925–14,945.
- Belardinelli, M. E., A. Bizzarri, and M. Cocco (2003), Earthquake triggering by static and dynamic stress changes, *J. Geophys. Res.*, *108*(B3), 2135, doi:10.1029/2002JB001779.
- Dieterich, J. H. (1979), Modeling of rock friction: 1. Experimental results and constitutive equations, *J. Geophys. Res.*, *84*, 2161–2168.
- Dieterich, J. H. (1987), Nucleation and triggering of earthquake slip: Effect of periodic stresses, *Tectonophysics*, *144*, 127–139.
- Dieterich, J. (1994), A constitutive law for rate of earthquake production and its application to earthquake clustering, *J. Geophys. Res.*, *99*, 2601–2618.
- Felzer, K. R., R. E. Abercrombie, and E. E. Brodsky (2003), Testing the stress shadow hypothesis, *Eos Trans. AGU*, *84*(46), Fall Meet. Suppl., Abstract S31A-04.
- Freed, A. M., and J. Lin (2001), Delayed triggering of the 1999 Hector Mine earthquake by viscoelastic stress transfer, *Nature*, *411*, 180–183.
- Gomberg, J. (2001), The failure of earthquake failure models, *J. Geophys. Res.*, *106*, 16,253–16,264.
- Gomberg, J., M. L. Blanpied, N. M. Beeler, and P. Bodin (1997), Transient triggering of near and distant earthquakes, *Bull. Seismol. Soc. Am.*, *87*, 294–309.
- Gomberg, J., N. M. Beeler, M. L. Blanpied, and P. Bodin (1998), Earthquake triggering by transient and static deformations, *J. Geophys. Res.*, *103*, 24,411–24,426.
- Gomberg, J., N. M. Beeler, and M. L. Blanpied (2000), On rate-and-state and Coulomb failure models, *J. Geophys. Res.*, *105*, 7857–7872.
- Gomberg, J., P. Reasenberg, N. Beeler, M. Cocco, and M. Belardinelli (2005), Time-dependent earthquake probabilities based on population models, *J. Geophys. Res.*, doi:10.1029/2004JB003405, in press.
- Gross, S. (2001), A model of tectonic stress state and rate using the 1994 Northridge earthquake sequence, *Bull. Seismol. Soc. Am.*, *91*, 263–275.
- Gross, S., and R. Burgmann (1998), Rate and state of background stress estimated from the aftershocks of the 1989 Loma Prieta, California earthquake, *J. Geophys. Res.*, *103*, 4915–4927.
- Gross, S., and C. Kisslinger (1997), Estimating tectonic stress rate and state with Landers aftershocks, *J. Geophys. Res.*, *102*, 7603–7612.
- Hardebeck, J. L. (2004), Stress triggering and earthquake probability estimates, *J. Geophys. Res.*, *109*, B04310, doi:10.1029/2003JB002437.
- Harris, R. A., and R. W. Simpson (1998), Suppression of large earthquakes by stress shadows: A comparison of Coulomb and rate-and-state failure, *J. Geophys. Res.*, *103*, 24,439–24,451.
- Helmstetter, A., and D. Sornette (2002), Subcritical and supercritical regimes in epidemic models of earthquake aftershocks, *J. Geophys. Res.*, *107*(B10), 2237, doi:10.1029/2001JB001580.
- Kilb, D., and A. M. Rubin (2002), Implications of diverse fault orientations imaged in relocated aftershocks of the Mount Lewis, M_L 5.7, California, earthquake, *J. Geophys. Res.*, *107*(B11), 2294, doi:10.1029/2001JB000149.
- Marsan, D. (2003), Triggering of seismicity at short timescales following Californian earthquakes, *J. Geophys. Res.*, *108*(B5), 2266, doi:10.1029/2002JB001946.

- Matthews, M. V., W. L. Ellsworth, and P. A. Reasenberg (2002), A Brownian model for recurrent earthquakes, *Bull. Seismol. Soc. Am.*, *92*, 2233–2250.
- Meade, B. J., and B. H. Hager (2004), Viscoelastic deformation for a clustered earthquake cycle, *Geophys. Res. Lett.*, *31*, L10610, doi:10.1029/2004GL019643.
- Nur, A., and J. R. Booker (1972), Aftershocks caused by pore fluid flow?, *Science*, *175*, 885–887.
- Ogata, Y., L. M. Jones, and S. Toda (2003), When and where the aftershock activity was depressed: Contrasting decay patterns of the proximate large earthquakes in southern California, *J. Geophys. Res.*, *108*(B6), 2318, doi:10.1029/2002JB002009.
- Pollitz, F., M. Vergnolle, and E. Calais (2003), Fault interaction and stress triggering of twentieth century earthquakes in Mongolia, *J. Geophys. Res.*, *108*(B10), 2503, doi:10.1029/2002JB002375.
- Rubin, A. M. (2002), Aftershocks of microearthquakes as probes of the mechanics of rupture, *J. Geophys. Res.*, *107*(B7), 2142, doi:10.1029/2001JB000496.
- Ruina, A. (1983), Slip instability and state variable friction laws, *J. Geophys. Res.*, *88*, 10,359–10,370.
- Scholz, C. H. (1968), Microfractures, aftershocks, and seismicity, *Bull. Seismol. Soc. Am.*, *58*, 1117–1130.
- Stein, R. S., A. A. Barka, and J. H. Dieterich (1997), Progressive failure on the North Anatolian fault since 1939 by earthquake stress triggering, *Geophys. J. Int.*, *128*, 594–604.
- Toda, S., and R. Stein (2003), Toggling of seismicity by the 1997 Kagoshima earthquake couplet: A demonstration of time-dependent stress transfer, *J. Geophys. Res.*, *108*(B12), 2567, doi:10.1029/2003JB002527.
- Toda, S., R. S. Stein, P. A. Reasenberg, J. H. Dieterich, and A. Yoshida (1998), Stress transferred by the 1995 $M_w = 6.9$ Kobe, Japan, shock: Effect on aftershocks and future earthquake probabilities, *J. Geophys. Res.*, *103*, 24,543–24,565.
- Utsu, T. (1961), A statistical study on the occurrence of aftershocks, *Geophys. Mag.*, *30*, 521–605.
- Ziv, A., A. M. Rubin, and D. Kilb (2003), Spatio-temporal analyses of earthquake productivity and size distribution: Observations and simulations, *Bull. Seismol. Soc. Am.*, *93*, 2069–2081.

M. E. Belardinelli, Settore di Geofisica, Dipartimento di Fisica, Università di Bologna, Viale Berti-Pichat 8, I-40127 Bologna, Italy. (elina@ibogfs.df.unibo.it)

M. Cocco, Istituto Nazionale di Geofisica e Vulcanologia, Via di Vigna Murata 605, I-00143 Rome, Italy. (cocco@ingv.it)

J. Gomberg, U.S. Geological Survey, 3876 Central Ave., Suite 2, Memphis, TN 38152, USA. (gomberg@usgs.gov)

P. Reasenberg, U.S. Geological Survey, MS 977, 345 Middlefield Road, Menlo Park, CA 92045, USA. (reasen@usgs.gov)